

A Critical Escape Probability Formulation for Enhancing the Transient Stability of Power Systems with System Parameter Design

Xian Wu^a, Kaihua Xi^a, Aijie Cheng^a, Chenghui Zhang^b, Hai Xiang Lin^{c,d}

^a*School of Mathematics, Shandong University, Jinan, 250100, P. R. China*

^b*School of Control Science and Engineering, Shandong University, Jinan, 250061, P. R. China*

^c*Delft Institute of Applied Mathematics, Delft University of Technology, Delft, 2628 CD, The Netherlands*

^d*Institute of Environmental Sciences (CML), Leiden University, Leiden 2333 CC, The Netherlands*

Abstract

For the enhancement of the transient stability of power systems, the key is to define a quantitative optimization formulation with system parameters as decision variables. In this paper, we model the disturbances by Gaussian noise and define a metric named *Critical Escape Probability* (CREP) based on the invariant probability measure of a linearised stochastic processes. CREP characterizes the probability of the state escaping from a critical set. CREP involves all the system parameters and reflects the size of the basin of attraction of the nonlinear systems. An optimization framework that minimizes CREP with the system parameters as decision variables is presented. Simulations show that the mean first hitting time when the state hits the boundary of the critical set, that is often used to describe the stability of nonlinear systems, is dramatically increased by minimizing CREP. This indicates that the transient stability of the system is effectively enhanced. It also shown that suppressing the state fluctuations only is insufficient for enhancing the transient stability. In addition, the famous Braess' paradox which also exists in power systems is revisited. Surprisingly, it turned out that the paradoxes identified by the traditional metric may not exist according to CREP. This new metric opens a new avenue for the transient stability analysis of future power systems integrated with large amounts of renewable energy.

Key words: invariant probability distribution, stochastic nonlinear power systems, first hitting time.

1 INTRODUCTION

In the synchronous state of a power system, the frequencies of all synchronous machine must be at or near the nominal frequency (eg, 50 Hz or 60 Hz). The frequency is the derivative of the rotational phase angle and is equal to the rotational speed of the synchronous machine expressed in units of rad/s. Synchronization of the frequency is essential for the proper functioning of a power system. Severe interference can cause desynchronization, which can lead to widespread power outages. Current energy systems are moving towards more distributed generation by renewables, which tend to be inherently more uncertain and low inertial, posing an even greater threat to synchrony.

Synchronization stability, which is also called *the transient stability* in power engineering, is the ability to maintain the synchronization when subjected to disturbances [9]. In this paper, we refer to synchronization stability and transient stability equivalently. The synchronous state and its stability are determined by the system parameters which include the power generation and loads, the inertia and the damping of the synchronous machines, the capacity of lines and the network topology. For deterministic systems, significant insights on the role of these parameters have been obtained from investigations on the existence condition of a synchronous state [5,4], the linear or nonlinear stability [14], the synchronization coherence [7] and the basin of attraction [13,3]. The system parameters may be assigned to optimize the synchrony, which can be obtained by load frequency control, the placement of virtual inertia, configuration of the damping coefficient, deletion or addition of lines or by changing the line capacities. In particular, regarding the transient stability, the local convergence to the synchronous state or the basin of attraction of the synchronous state are investigated [1,28].

* Corresponding author: Kaihua Xi.

Email addresses: xianwu@mail.sdu.edu.cn (Xian Wu), kxi@sdu.edu.cn (Kaihua Xi), aijie@sdu.edu.cn (Aijie Cheng), zchui@sdu.edu.cn (Chenghui Zhang), H.X.Lin@tudelft.nl (Hai Xiang Lin).

In practice, the synchronous state of the power system is a set point for control, in which control actions are taken to let the state converge to this set point after disturbances. Thus, with frequently occurring disturbances, e.g., the uncertainties from wind energy and power demand and unpredictable fault in power generation, the frequency, and the phase usually fluctuate around the synchronous state. If both the fluctuations of the frequency and phase difference between the synchronous machines are so large that the state of the system cannot return to the synchronous state, then the synchronization is lost. Hence, the risk of losing synchronization is actually determined by two factors, i.e., the size of the basin of attraction of the synchronous state and the fluctuation of the state caused by the disturbances. To increase the transient stability, it is important to find such a synchronous state that has a large basin of attraction and around which the fluctuation of the state is also small. It is insufficient to analyze the transient stability in a deterministic system without considering the state fluctuations caused by the disturbances.

Regarding the state fluctuations, various investigations have been made to learn the impacts of the system parameters, from which insights have been obtained on the propagation of the disturbances and the parameter assignment for suppressing the fluctuations. With perturbations added to the system parameters, the disturbance arrival time is estimated in [30]. The amplitude of perturbation responses of the nodes is used to study the emergent complex response patterns across the network in [29]. By modelling the disturbances as inputs to an associated linearized system, the fluctuations are evaluated by the \mathcal{H}_2 norm of the input-output linear system [6,15,19]. By minimizing it, the fluctuations can also be effectively suppressed by system parameter assignment, such as the optimal placement of virtual inertia [15]. To precisely characterize the fluctuations, the variances of the frequency at each node and the phase difference at each line in the invariant probability distribution are investigated [21,?] with the disturbance modelled by Gaussian noise. It is found that the impacts of the disturbances at the nodes can be described by the *Superposition Principle* [24]. With assumption of uniform disturbance-damping ratios among the nodes, explicit formulas of the variance have been deduced. From these formulas it is found that the fluctuations are related to the cycle space of graphs [21]. In control theory, the robust control method is applicable to suppress the fluctuations by controlling the power generation in load frequency control. However, for enhancing the transient stability, it is insufficient to suppress the fluctuations only because the stability also depends on the basin of attraction.

For enhancing the transient stability, the most difficult problem is to define a quantitative optimization formulation with the system parameters as the decision variables. The mean of the first hitting time when the state

hits the boundary of the basin of attraction is often used to study the survival time of a system, which is also used to study the stability of non-linear systems[11,8]. The longer is the mean first hitting time, the more stable is the system under stochastic disturbances. Both of the basin of attraction and the severity of the state fluctuations are involve into this value, which makes it a potential metric for the transient stability. However, it can hardly be maximized directly because it is difficult to get the probability distribution of the first hitting time and the boundary of the basin of attraction. For coupled phase oscillators, the probability that the state exits a secure domain, which also involves the basin of attraction and the state fluctuations, is investigated in order to enhance the synchronization stability of the system in [23]. However, the dynamics of the frequencies at the nodes are not considered in that system.

In this paper, for power systems with stochastic disturbances, we model the disturbances by Gaussian noises and focus on the invariant probability distribution of the frequency and the phase difference in a linearized stochastic process. We define a metric named *Critical Escape Probability*(CREP), which describes the probability of the state escaping from a critical set, to assess the transient stability. It is related to the mean first hitting time of the state to the boundary of the critical set, i.e., the smaller is CREP, the longer is the mean first hitting time. We analyze the trends of CREP as the system parameters change and its relationship to the size of the basin of attraction. In addition, we revisit the famous Braess' paradox [22,2] with CREP. It is found this paradox can also be identified by CREP. In particular, it is surprisingly found that adding a new line may lead to increasing the stability under CREP while decreasing the stability under the other existing metrics. This is because the influences of all the system parameters are included into CREP while in the other metrics, e.g., the linear stability measured by the spectrum of the Jacobi matrix and the order parameter defined by Kuramoto to study the level of the synchronization, not all system parameter's influences are fully considered. We formulate an optimization framework that minimizes CREP with the system parameters as decision variables. The mean first hitting time is used to verify the performance of CREP on identifying the Braess' paradox and the optimization framework on enhancing the transient stability. The optimization framework can be applied in optimal power flow calculation, the placement of virtual inertia, tuning the gain for droop control and the design of the network topology. It also provides a new avenue to the stability analysis of the complex system in which the synchronization plays an important role on the proper function of the system [5].

The contributions of this paper include:

- (1) CREP formulation for assessing the transient stability, which involves the roles of all the system param-

eters and can be minimized to enhance the transient stability;

- (2) An optimization framework that minimizes CREP, by which the system parameters can be optimally configured to increase the first hitting time, thus enhance the transient stability of the system under stochastic disturbances;
- (3) A new finding on the identification of the Braess' paradox by CREP.

This paper is organized as follows. We formulate the problem by introducing the mathematical model of power system and the concept of the mean first hitting time in Section 2. The invariant probability distribution of a linear stochastic process and the definition of CREP are described in Section 3 and the optimization framework for improving the transient stability is presented in Section 4. We analyze the dependence of CREP on the system parameters and evaluate performance of the proposed optimization framework on improving the transient stability through case studies in Section 5 and conclude with remarks in Section 6.

2 Problem formulation

In this section, we present the scientific problem of this paper with the introduction of the model and the mean first hitting time of a stochastic process.

2.1 The model

The network of the power system can be modelled by a graph $\mathcal{G} = (\mathcal{V}, \mathcal{E})$ with n nodes in set \mathcal{V} and m lines in set $\mathcal{E} \subset \mathcal{V} \times \mathcal{V}$, where a node denotes a bus and a line denotes a transmission line connecting two buses. We focus on the transmission network and assume the lines are lossless. The dynamics of the power system are described by the swing equations [28,12,1]

$$\dot{\delta}_i(t) = \omega_i(t), \quad (1a)$$

$$m_i \dot{\omega}_i(t) = P_i - d_i \omega_i(t) - \sum_{j=1}^n l_{i,j} \sin(\delta_i(t) - \delta_j(t)), \quad (1b)$$

where $\delta_i(t)$ and $\omega_i(t)$ denote the phase angle and the frequency deviation from the nominal frequency of the synchronous machine at node i ; $m_i > 0$ describes the inertia of the synchronous generators; $d_i > 0$ represents the damping coefficient with droop control; P_i denotes power generation if $P_i > 0$ and denotes power load otherwise; $l_{i,j} = \hat{b}_{i,j} V_i V_j$ is the effective susceptance, where $\hat{b}_{i,j}$ is the susceptance of the line (i, j) and V_i is the voltage. In this paper, $l_{i,j}$ is also referred as the *line capacity*. We assume that the voltage at each node is a constant because the dynamics of the voltage and that of the frequency can be decoupled in the stability analysis (1).

It is assumed that the graph is connected, thus it holds $m > n - 1$.

When the power generations and loads are time invariant, the frequencies at the nodes synchronize at an equilibrium state, called *the synchronous state* that satisfies, for $i = 1, 2, \dots, n$,

$$\omega_i(t) = \omega_{syn} \quad \text{and} \quad \omega_{syn} - \frac{\sum_{i=1}^n P_i}{\sum_{i=1}^n d_i} = 0.$$

Without loss of generality, we assume $\sum_{i=1}^n P_i = 0$, which means that the power generations and loads are balanced. In practice, this balance is achieved by secondary frequency control [26]. Hence, at the synchronous state, it holds that $\omega_{syn} = 0$, and the phases δ_i^* at the nodes satisfies,

$$P_i - \sum_{j=1}^n l_{i,j} \sin(\delta_i^* - \delta_j^*) = 0. \quad (2)$$

Clearly, the existence of a synchronous state depends on the topology structure, the distribution of power generations and loads at each node and the line capacities [5,4]. Denote the synchronous state by $((\boldsymbol{\delta}^*)^\top, \mathbf{0})^\top \in \mathbb{R}^{2n}$ with $\boldsymbol{\delta}^* = \text{col}(\delta_i^*) \in \mathbb{R}^n$. For practical reasons, we restrict our attention to the synchronous state with the phase in the following domain

$$\Theta_\delta = \{\boldsymbol{\delta} \in \mathbb{R}^n \mid |\delta_i - \delta_j| < \pi/2, \forall (i, j) \in \mathcal{E}\}. \quad (3)$$

It has been proven there exists at most one synchronous state in this domain and when it exists, it is asymptotically stable [17]. The stability region of the synchronous state has been analyzed by [1] and independently by [28].

In real networks, the state of the power system always fluctuates around the synchronous state due to various disturbances. When the fluctuations are very large, the state may exit the stability region of the synchronous state and become unstable. Desynchronization means that both the fluctuations of the frequency and the phase angle difference are so large that the system cannot return to the synchronous state. The fluctuations depend on many factors, which include the line capacity, the inertia and damping of the synchronous machines, the network topology and the strength of disturbances. The source of the disturbances are also various, e.g., the renewable power generation, fault of the devices in the network, etc. We focus on the following problem.

Problem 2.1 *How to improve the transient stability of the system under stochastic disturbances by changing the system parameters?*

To address this problem, we model the disturbance by Gaussian noise and focus on the following stochastic pro-

cess,

$$d\delta_i(t) = \omega_i(t)dt, \quad (4a)$$

$$m_i d\omega_i(t) = (P_i - d_i \omega_i(t) - \sum_{j=1}^n l_{i,j} \sin(\delta_{ij}(t)))dt + b_i dv_i(t), \quad (4b)$$

where $\delta_{ij}(t) = \delta_i(t) - \delta_j(t)$, b_i is used to describe the strength of the noise, $v_i(t)$ is a Brownian motion process, which has increments with a Gaussian probability distribution. Here, we have assumed for any two distinct nodes i and j the stochastic process $v_i(t)$ and $v_j(t)$ are independent. This is reasonable because the locations of the renewable power generators with serious power generation uncertainties are usually far from each other.

Denote $e_k = (i, j) \in \mathcal{E}$ for $k = 1, \dots, m$. To obtain the information of the frequency and the phase difference, we define the output of the system (1) as the frequencies at the nodes and the phase differences in the lines as follows,

$$\mathbf{y}(t) = \mathbf{C}\mathbf{x}(t), \mathbf{x}(t) = \begin{bmatrix} \boldsymbol{\delta}(t) \\ \boldsymbol{\omega}(t) \end{bmatrix}, \mathbf{y}(t) = \begin{bmatrix} \mathbf{y}_\delta(t) \\ \mathbf{y}_\omega(t) \end{bmatrix}, \mathbf{C} = \begin{bmatrix} \tilde{\mathbf{C}}^\top & \mathbf{0} \\ \mathbf{0} & \mathbf{I}_n \end{bmatrix},$$

where $\mathbf{y} \in \mathbb{R}^{n+m}$, $\mathbf{C} \in \mathbb{R}^{(m+n) \times 2n}$, $\mathbf{x} \in \mathbb{R}^{2n}$, $\boldsymbol{\delta} = \text{col}(\delta_i) \in \mathbb{R}^n$, $\boldsymbol{\omega} = \text{col}(\omega_i) \in \mathbb{R}^n$, $\mathbf{y}_\delta = \text{col}(y_{\delta_k}) \in \mathbb{R}^m$ with $y_{\delta_k} = \delta_i - \delta_j$ for $k = 1, \dots, m$, $\mathbf{y}_\omega = \boldsymbol{\omega} \in \mathbb{R}^n$, $\tilde{\mathbf{C}} = (C_{ik}) \in \mathbb{R}^{n \times m}$ is the incidence matrix of graph \mathcal{G} such that

$$C_{i,k} = \begin{cases} 1, & \text{if node } i \text{ is the beginning of line } e_k, \\ -1, & \text{if node } i \text{ is the end of line } e_k, \\ 0, & \text{otherwise,} \end{cases} \quad (5)$$

where the direction of line e_k is specified arbitrarily without influence on the study below, $\mathbf{I}_n \in \mathbb{R}^{n \times n}$ is an identity matrix. Note that the first m elements of \mathbf{y} are the phase differences in the m lines and the next n elements are the frequencies at the n nodes. At the synchronous state $\mathbf{x}^* = ((\boldsymbol{\delta}^*)^\top, \mathbf{0})^\top$, the output becomes

$$\mathbf{y}^* = \mathbf{C}\mathbf{x}^* = ((\tilde{\mathbf{C}}^\top \boldsymbol{\delta}^*)^\top, \mathbf{0})^\top. \quad (6)$$

To address Problem 2.1, a metric that fully reflect the transient stability and can be minimized or maximized as an objective function in an optimization problem is sought. The mean first hitting time that is often used to describe the stability of a nonlinear system is introduced below.

Definition 2.2 Consider a stochastic process $\{\mathbf{x}(t) \in \mathbb{X}, t \in \mathbb{T}\}$ with initial state $\mathbf{x}(0) = \mathbf{x}_0$ and a boundary set \mathbb{B} of set \mathbb{A} , in which $\mathbb{A} \subset \mathbb{X}$ and $\mathbb{T} = [0, +\infty)$. Assume that the initial value \mathbf{x}_0 of the process lies inside \mathbb{A} but outside

\mathbb{B} , then the first hitting time is defined by the random variable $t_e : \Omega \rightarrow \mathbb{R} \cup \{+\infty\}$,

$$t_e = \begin{cases} \inf_{t \in \mathbb{T}} \mathbf{x}(t) \in \mathbb{B}, & \text{if such a } t \in \mathbb{R} \text{ exists,} \\ +\infty, & \text{else,} \end{cases}$$

where t_e is the first time when the sample path of the stochastic process reaches the boundary set \mathbb{B} .

The first hitting time is also called *the first exit time* of the set \mathbb{A} with boundary set \mathbb{B} . It is a random variable and a stopping time of the σ algebra family generated by the process $\mathbf{x}(t)$. We denote the mean of t_e by \bar{t}_e . It is obvious that the first hitting time depends on the initial state $\mathbf{x}(0)$, the probability distribution of $\mathbf{x}(t)$ and the boundary set \mathbb{B} .

In reality, the stability depends on how the system reacts to a series of small fluctuations. If we set $\mathbb{B} = \partial\mathbb{A}$, with the set \mathbb{A} is the basin of attraction, and the initial state as the synchronous state, the expectation of the first hitting time of the process $(\boldsymbol{\delta}(t)^\top, \boldsymbol{\omega}(t)^\top)^\top$ in (4) can fully reflect the transient stability, i.e., this expectation depends on the size of the basin of attraction and the strength of the disturbances. This makes it a potential candidate for the metric. However, the distribution of the first hitting time can hardly be derived analytically or even approximated by the Monte-Carlo method because of the difficulty on describing the boundary of the basin of attraction. Due to this difficulty, we set $\mathbb{X} = \Theta$,

$$\Theta = \Theta_\delta \times \Theta_\omega, \quad (7)$$

with Θ_δ is defined in (3) and

$$\Theta_\omega = \{\boldsymbol{\omega} \in \mathbb{R}^n \mid |\omega_i| < \epsilon, \forall i \in \mathcal{V}\}, \quad (8)$$

where $\epsilon \in \mathbb{R}$ is a small real number corresponding to the quality of power supply according to the requirement of governments, i.e., the frequency fluctuation should be sufficiently small to guarantee the system stability. If the state goes out of this set, the synchronization may be lost. The set Θ is critical for monitoring the transient stability [27], Hence, we call it a *critical set* for the transient stability of the system in this paper.

Let us reconsider the synchronization of the system (1) under the disturbances. With the definition of t_e and $\mathbb{X} = \Theta$, the state $\mathbf{x}(t)$ of the system (4) remains in the set Θ in the period $[0, t_e]$, i.e., $\mathbf{x}(t) \in \Theta$ for any $t \in [0, t_e]$, thus the synchronization is maintained in the period $[0, t_e]$. Once the state exits the set Θ , the synchronization may be lost. If $t_e \rightarrow +\infty$, desynchronization will almost never happen under the disturbances. Thus, the larger is t_e , the longer is the time that the synchronization is maintained, which means the synchronization is more stable under the disturbances. This makes the mean first

hitting time \bar{t}_e a suitable metric for the transient stability. Clearly, the mean \bar{t}_e can be approximated by the Monte-Carlo method with simulations of (4), thus can be used to assess the transient stability. However, to maximize \bar{t}_e in an optimization problem, one has to know the analytical expression of its probability distribution, which can hardly be derived because of the high dimension and nonlinearity of the system (4). Thus, an alternative metric for enhancing the transient stability by an optimization framework has to be designed.

3 CREP for transient stability

In this section, we define a metric that can be minimized as an optimization problem with the system parameters as decision variables for enhancing the transient stability.

An intuitive way to increase \bar{t}_e is to increase the probability of the state $\mathbf{x}(t)$ staying in the critical set Θ . This is equivalent to increasing the probability of the output $\mathbf{y}(t)$ staying in the set

$$\begin{aligned}\Theta_y &= \Theta_{y_\delta} \times \Theta_\omega, \\ \Theta_{y_\delta} &= \{\mathbf{y}_\delta \in \mathbb{R}^m \mid |y_k| < \pi/2, \forall e_k = (i, j) \in \mathcal{E}\}.\end{aligned}$$

Due to the nonlinearity and the high dimension of the state of the system (4), the probability distribution of the process $\mathbf{y}(t)$ can hardly be analytically obtained. Because the state $\mathbf{x}(t)$ always fluctuates around the synchronous state $\mathbf{x}^* = ((\boldsymbol{\delta}^*)^\top, \mathbf{0})^\top$, the output $\mathbf{y}(t) = \mathbf{C}\mathbf{x}(t)$ fluctuates around the value $\mathbf{y}^* = \mathbf{C}\mathbf{x}^*$, which is seen as the expectation of the output. To investigate the fluctuations, the system (4) is linearised around the synchronous state $\mathbf{x}^* = ((\boldsymbol{\delta}^*)^\top, \mathbf{0})$,

$$d\widehat{\mathbf{x}}(t) = \mathbf{A}\widehat{\mathbf{x}}(t)dt + \mathbf{B}d\mathbf{v}(t), \quad (9a)$$

$$\widehat{\mathbf{y}}(t) = \mathbf{C}\widehat{\mathbf{x}}(t), \quad (9b)$$

with the state variable, output vector, system matrix and input matrix

$$\begin{aligned}\widehat{\mathbf{x}}(t) &= \begin{bmatrix} \widehat{\boldsymbol{\delta}}(t) \\ \widehat{\boldsymbol{\omega}}(t) \end{bmatrix}, \quad \widehat{\mathbf{y}}(t) = \begin{bmatrix} \widehat{\mathbf{y}}_\delta(t) \\ \widehat{\mathbf{y}}_\omega(t) \end{bmatrix}, \\ \mathbf{A} &= \begin{bmatrix} \mathbf{0} & \mathbf{I}_n \\ -\mathbf{M}^{-1}\mathbf{L}_c & -\mathbf{M}^{-1}\mathbf{D} \end{bmatrix}, \quad \mathbf{B} = \begin{bmatrix} \mathbf{0} \\ \mathbf{M}^{-1}\widetilde{\mathbf{B}} \end{bmatrix}, \quad \mathbf{C} = \begin{bmatrix} \widetilde{\mathbf{C}}^\top & \mathbf{0} \\ \mathbf{0} & \mathbf{I}_n \end{bmatrix},\end{aligned}$$

where $\widehat{\mathbf{x}}$ represents the deviation of the state $\mathbf{x}(t)$ from the synchronous state \mathbf{x}^* , $\mathbf{v}(t) = \text{col}(v_i(t)) \in \mathbb{R}^n$, $\mathbf{M} = \text{diag}(m_i)$, $\mathbf{D} = \text{diag}(d_i)$, $\widetilde{\mathbf{B}} = \text{diag}(b_i)$ are diagonal matrices, \mathbf{L}_c is a singular Laplacian matrix whose elements satisfy

$$l_{cij} = \begin{cases} -l_{i,j} \cos(\delta_i^* - \delta_j^*), & i \neq j, \\ \sum_{k \neq i} l_{i,k} \cos(\delta_i^* - \delta_k^*), & i = j. \end{cases}$$

The matrix \mathbf{A} is also called the *Jacobian matrix* of the system (1) at the synchronous state $((\boldsymbol{\delta}^*)^\top, \mathbf{0})^\top$. Because of the Gaussian distribution of $\mathbf{v}(t)$, the process $\widehat{\mathbf{x}}$ and $\widehat{\mathbf{y}}(t)$ are also Gaussian such that

$$\widehat{\mathbf{x}}(t) \in G(\mathbf{m}_{\widehat{\mathbf{x}}}(t), \mathbf{Q}_{\widehat{\mathbf{x}}}(t)), \quad \widehat{\mathbf{y}}(t) \in G(\mathbf{m}_{\widehat{\mathbf{y}}}(t), \mathbf{Q}_{\widehat{\mathbf{y}}}(t)).$$

with $\mathbf{m}_{\widehat{\mathbf{x}}}(t) \in \mathbb{R}^{2n}$ and $\mathbf{m}_{\widehat{\mathbf{y}}}(t) \in \mathbb{R}^{m+n}$, $\mathbf{Q}_{\widehat{\mathbf{x}}}(t) \in \mathbb{R}^{2n \times 2n}$ and $\mathbf{Q}_{\widehat{\mathbf{y}}}(t) \in \mathbb{R}^{(m+n) \times (m+n)}$.

In real networks, the state always fluctuates around the synchronous state under various disturbances. Thus, it is reasonable to use the variance of $\widehat{\mathbf{x}}(t)$ in the invariant probability distribution, regardless the initial probability distribution of $\widehat{\mathbf{x}}(t)$, to measure the fluctuations [21].

Because the system matrix \mathbf{A} is singular, the invariant probability distribution of $\widehat{\mathbf{x}}(t)$ does not exist. However, the invariant probability distribution of $\widehat{\mathbf{y}}(t)$ exists [21], i.e.,

$$\lim_{t \rightarrow \infty} \mathbf{m}_{\widehat{\mathbf{y}}}(t) = \mathbf{0}, \quad \lim_{t \rightarrow \infty} \mathbf{Q}_{\widehat{\mathbf{y}}}(t) = \mathbf{Q}_{\widehat{\mathbf{y}}}.$$

With this Gaussian process, we further define a new process to approximate the process $\mathbf{y}(t)$.

Definition 3.1 *Given the output \mathbf{y}^* in (6) and the Gaussian process $\widehat{\mathbf{y}}(t)$ in (9), the stochastic process $\widetilde{\mathbf{y}}(t)$ is defined as,*

$$\widetilde{\mathbf{y}}(t) = \widehat{\mathbf{y}}(t) + \mathbf{y}^*. \quad (10)$$

We denote $\widetilde{\mathbf{y}}(t) = (\widetilde{\mathbf{y}}_\delta^\top(t), \widetilde{\mathbf{y}}_\omega^\top(t))^\top$. The process $\widetilde{\mathbf{y}}(t)$ is Gaussian process,

$$\widetilde{\mathbf{y}}(t) \in G(\mathbf{m}_{\widetilde{\mathbf{y}}}(t), \mathbf{Q}_{\widetilde{\mathbf{y}}}(t))$$

and has invariant probability distribution with

$$\lim_{t \rightarrow \infty} \mathbf{m}_{\widetilde{\mathbf{y}}}(t) = \mathbf{y}^*, \quad \lim_{t \rightarrow \infty} \mathbf{Q}_{\widetilde{\mathbf{y}}}(t) = \mathbf{Q}_{\widetilde{\mathbf{y}}}.$$

Clearly, $\widetilde{\mathbf{y}}(t)$ also fluctuates around \mathbf{y}^* . It actually approximates $\mathbf{y}(t)$ at the neighborhood of \mathbf{y}^* because the linearisation of the system (4) at the synchronous state $\mathbf{x}^* = ((\boldsymbol{\delta}^*)^\top, \mathbf{0})^\top$.

With \mathbf{y}^* as the expectation solved from (2) and the variance matrix $\mathbf{Q}_{\widetilde{\mathbf{y}}}$, the probability that the process $\widetilde{\mathbf{y}}(t)$ is in the set Θ at the invariant probability distribution can be calculated. However, this probability still can hardly be computed because an integral over a supercube of dimension $m+n$ is needed, which involves immense computational complexity. Thus, we focus on the marginal probability distribution of the components of $\widetilde{\mathbf{y}}(t)$ in the invariant probability distribution. Denote the vector formed by the diagonal elements of

the matrix $\mathbf{Q}_{\tilde{\mathbf{y}}}$ by $\boldsymbol{\sigma}^2 = ((\boldsymbol{\sigma}_\delta^2)^\top, (\boldsymbol{\sigma}_\omega^2)^\top)^\top \in \mathbb{R}^{n+m}$ where $\boldsymbol{\sigma}_\delta^2 = \text{col}(\sigma_{\delta_k}^2) \in \mathbb{R}^m$ and $\boldsymbol{\sigma}_\omega^2 = \text{col}(\sigma_{\omega_j}^2) \in \mathbb{R}^n$ are the variances of the phase differences in the lines and the frequencies at the nodes. It is noticed that σ_{δ_k} and σ_{ω_j} are the standard variances of the phase difference in line e_k and the frequency at node j respectively. The logic behind enhancing the transient stability is to increase the probability of $\mathbf{y}(t)$ in the domain Θ_y . With this logic, we define a critical escape probability based on the invariant marginal probability distribution of the components of $\tilde{\mathbf{y}}(t)$ as below.

Definition 3.2 Consider the stochastic process $\tilde{\mathbf{y}}(t)$ in (10). Denote $\mathbf{f} = (\mathbf{f}_\delta^\top, \mathbf{f}_\omega^\top)^\top \in \mathbb{R}^{n+m}$ and $\mathbf{f}_\delta = \text{col}(f_{\delta_k}) \in \mathbb{R}^m$ and $\mathbf{f}_\omega = \text{col}(f_{\omega_k}) \in \mathbb{R}^n$ with f_{δ_k} and f_{ω_k} defined as the probability of the absolute values of \tilde{y}_{δ_k} and \tilde{y}_{ω_k} exiting $\pi/2$ and ϵ such that

$$f_{\delta_k} = 1 - \int_{-\pi/2}^{\pi/2} \frac{1}{\sqrt{2\pi}\sigma_{\delta_k}} e^{-\frac{(z-y_k^*)^2}{2\sigma_{\delta_k}^2}} dz, \quad (11)$$

$$f_{\omega_k} = 1 - \int_{-\epsilon}^{\epsilon} \frac{1}{\sqrt{2\pi}\sigma_{\omega_k}} e^{-\frac{z^2}{2\sigma_{\omega_k}^2}} dz, \quad (12)$$

respectively. The Critical Escape Probability (CREP) assessing the probability of $\tilde{\mathbf{y}}(t)$ escaping from the set Θ_y in the invariant probability distribution is defined as

$$\Phi = \|\mathbf{f}\|_\infty, \quad (13)$$

Analogously, the CREP assessing the probability of $\tilde{\mathbf{y}}_\delta(t)$ escaping from the set Θ_δ and the probability of $\tilde{\mathbf{y}}_\omega(t)$ escaping from the set Θ_ω are respectively defined as

$$\Phi_\delta = \|\mathbf{f}_\delta\|_\infty, \quad \Phi_\omega = \|\mathbf{f}_\omega\|_\infty.$$

Because $\tilde{\mathbf{y}}(t)$ approximates $\mathbf{y}(t)$ at the neighborhood of \mathbf{y}^* , by minimizing Φ , the probability of $\mathbf{y}(t)$ escaping from the critical set Θ decreases, which leads to an enhancement of the transient stability. Naturally, Φ is a metric effectively assessing the transient stability of the system (1) with stochastic disturbances. Similarly, when the rotor angle stability which focuses on the ability of the system to maintain the cohesiveness of the phase angles, and the frequency stability which considers the severity of the frequency fluctuations need to be enhanced separately, Φ_δ and Φ_ω can be minimized respectively. Clearly the performance of these minimization can be evaluated by the mean first hitting time of $\mathbf{y}(t)$ to the boundary $\partial\Theta_y$, which is approximated by the Monte-Carlo method with simulations of the nonlinear stochastic system (4).

Obviously, if ϵ in (12), which is a tolerance of the frequency fluctuations, is very large such that $\|\mathbf{f}_\delta\|_\infty > \|\mathbf{f}_\omega\|_\infty$, then $\Phi = \Phi_\delta$. On the other hand, if ϵ is very small such that $\|\mathbf{f}_\delta\|_\infty \leq \|\mathbf{f}_\omega\|_\infty$, then $\Phi = \Phi_\omega$.

We next present the procedure for calculating Φ and then introduce the characteristics of Φ .

The phase difference in the vector \mathbf{y}^* is solved from the power flow equation (2). For the calculation of $\boldsymbol{\sigma}$, we need to solve the variance matrix $\mathbf{Q}_{\tilde{\mathbf{y}}}$ for the system (9) which is presented below.

Because the Laplacian matrix \mathbf{L}_c is symmetric, singular and semi-positive definite, we have the following lemma.

Lemma 3.3 Consider the Laplacian matrix \mathbf{L}_c and the positive-definite diagonal matrix \mathbf{M} in system (9). There exists an orthogonal matrix $\mathbf{U} \in \mathbb{R}^{n \times n}$ such that

$$\mathbf{U}^\top \mathbf{M}^{-1/2} \mathbf{L}_c \mathbf{M}^{-1/2} \mathbf{U} = \boldsymbol{\Lambda}_n, \quad (14)$$

where $\boldsymbol{\Lambda}_n = \text{diag}(\lambda_i) \in \mathbb{R}^{n \times n}$ with $0 = \lambda_1 < \lambda_2 \cdots < \lambda_n$ being the eigenvalues of the matrix $\mathbf{M}^{-1/2} \mathbf{L}_c \mathbf{M}^{-1/2}$, $\mathbf{U} = [\mathbf{u}_1 \ \mathbf{u}_2 \ \cdots \ \mathbf{u}_n]$ with $\mathbf{u}_i \in \mathbb{R}^n$ being the eigenvector corresponding to λ_i for $i = 1, \dots, n$. In addition, $\mathbf{u}_1 = 1/\sqrt{n}\mathbf{1}_n$.

Based on Lemma 3.3, we have the following theorem [21].

Theorem 3.4 Consider the stochastic system (9) and the notations of matrices in Lemma 3.3. Define matrices

$$\begin{aligned} \mathbf{A}_e &= \begin{bmatrix} \mathbf{0} & \mathbf{I}_n \\ -\boldsymbol{\Lambda}_n & -\mathbf{U}^\top \mathbf{M}^{-1} \mathbf{D} \mathbf{U} \end{bmatrix} \in \mathbb{R}^{2n \times 2n}, \\ \mathbf{B}_e &= \begin{bmatrix} \mathbf{0} \\ \mathbf{U}^\top \mathbf{M}^{-\frac{1}{2}} \tilde{\mathbf{B}} \end{bmatrix} \in \mathbb{R}^{2n \times n}, \\ \mathbf{C}_e &= \begin{bmatrix} \tilde{\mathbf{C}}^\top \mathbf{M}^{-\frac{1}{2}} \mathbf{U} & \mathbf{0} \\ \mathbf{0} & \mathbf{M}^{-\frac{1}{2}} \mathbf{U} \end{bmatrix} \in \mathbb{R}^{(m+n) \times 2n}, \end{aligned} \quad (15)$$

which can be reformulated in blocks according to

$$\mathbf{A}_e = \begin{bmatrix} \mathbf{0} & \mathbf{A}_{12} \\ \mathbf{0} & \mathbf{A}_2 \end{bmatrix}, \quad \mathbf{B}_e = \begin{bmatrix} \mathbf{0} \\ \mathbf{B}_2 \end{bmatrix}, \quad \mathbf{C}_e = \begin{bmatrix} \mathbf{0} & \mathbf{C}_2 \end{bmatrix}, \quad (16)$$

where $\mathbf{A}_{12} \in \mathbb{R}^{1 \times (2n-1)}$, $\mathbf{A}_2 \in \mathbb{R}^{(2n-1) \times (2n-1)}$, $\mathbf{B}_2 \in \mathbb{R}^{(2n-1) \times 2n}$, and \mathbf{C}_2 is the matrix obtained by removing the first column of the matrix \mathbf{C}_e so that

$$\mathbf{C}_2 = \begin{bmatrix} \tilde{\mathbf{C}}^\top \mathbf{M}^{-1/2} \hat{\mathbf{U}} & \mathbf{0} \\ \mathbf{0} & \mathbf{M}^{-1/2} \mathbf{U} \end{bmatrix} \in \mathbb{R}^{(m+n) \times (2n-1)}, \quad (17)$$

with $\hat{\mathbf{U}} = [\mathbf{u}_2 \ \mathbf{u}_3 \ \cdots \ \mathbf{u}_n] \in \mathbb{R}^{n \times (n-1)}$. The variance matrix $\mathbf{Q}_{\tilde{\mathbf{y}}}$ of the output \mathbf{y} of the system (4) in the invariant probability distribution satisfies

$$\mathbf{Q}_{\tilde{\mathbf{y}}} = \mathbf{C}_2 \mathbf{Q}_{\tilde{\mathbf{x}}} \mathbf{C}_2^\top, \quad (18)$$

where $\mathbf{Q}_{\hat{x}} = \int_0^\infty e^{A_2 t} \mathbf{B}_2 \mathbf{B}_2^\top e^{A_2^\top t} dt \in \mathbb{R}^{(2n-1) \times (2n-1)}$ that is the unique solution of the following Lyapunov equation

$$\mathbf{A}_2 \mathbf{Q}_{\hat{x}} + \mathbf{Q}_{\hat{x}} \mathbf{A}_2^\top + \mathbf{B}_2 \mathbf{B}_2^\top = \mathbf{0}. \quad (19)$$

See [21] for the proof of this theorem. Based on Theorem 3.4, we present the procedure for the calculation of Φ .

Procedure 3.5 *The procedure for the calculation of the metric Φ ,*

- (1) Solve the power flow equation (2) for the synchronous state $\mathbf{x}^* = ((\delta^*)^\top, \mathbf{0})^\top$ and output $\mathbf{y}^* = \mathbf{C} \mathbf{x}^*$;
- (2) Derive the stochastic process (9) by linearising the system (1) at the synchronous state \mathbf{x}^* and model the disturbances by Gaussian noise;
- (3) Perform the spectral decomposition of the matrix \mathbf{L}_c in Lemma 3.3 and determine the matrices $\mathbf{A}_2, \mathbf{B}_2$ and \mathbf{C}_2 in Theorem 3.4;
- (4) Solve the Lyapunov equation (19) for the matrix $\mathbf{Q}_{\hat{x}}$ and calculate the matrix $\mathbf{Q}_{\hat{y}}$ according to (18);
- (5) Calculate the vector \mathbf{f} according to Definition 3.2 using the values of \mathbf{y}^* and the diagonal element σ^2 of $\mathbf{Q}_{\hat{y}}$,
- (6) Calculate the norm $\|\mathbf{f}\|_\infty$.

Clearly, Φ_δ and Φ_ω can be calculated at the same time with Φ by this procedure. An important observation is that using the value of \mathbf{f} , the line where the system loses synchronization the most easily and the node where the frequency fluctuation is the most severe can be identified. These identifications allow for the discovery of weak parts in the network that may lead to network desynchronization.

CREP Φ has the following characteristics.

- (i) CREP includes the influences of all the system parameters, the inertia and the damping of the synchronous machines, the distribution of the power loads and generation, the line capacity, the network topology and the strength of the disturbances.
- (ii) CREP also reflects the size of the basin of attraction and characterizes the phenomenon that the size of the basin shrinks if either the power flows in lines increase or if a line capacity decreases

The first characteristic is concluded directly from the calculation of \mathbf{f} and Φ in Procedure 3.5. Before explaining the second characteristic in a proposition, we first introduce a lemma for the bounds of the matrix $\mathbf{Q}_{\hat{y}}$, which is needed in the proof of the proposition. For matrices $\mathbf{A}, \mathbf{B} \in \mathbb{R}^{n \times n}$, we say that $\mathbf{A} \leq \mathbf{B}$ if the matrix $\mathbf{A} - \mathbf{B}$ is semi-negative-definite. To emphasize the variance matrix of the frequencies and the phase differences, we write

the matrix $\mathbf{Q}_{\hat{y}}$ in the following form,

$$\mathbf{Q}_{\hat{y}} = \begin{bmatrix} \mathbf{Q}_{\hat{\delta}} & \mathbf{Q}_{\hat{\delta}\hat{\omega}}^\top \\ \mathbf{Q}_{\hat{\delta}\hat{\omega}} & \mathbf{Q}_{\hat{\omega}} \end{bmatrix} \in \mathbb{R}^{(m+n) \times (m+n)}. \quad (20)$$

Lemma 3.6 *Consider the stochastic process (9). Define $\bar{\eta} = \max\{\eta_i, i = 1, \dots, n\}$ and $\underline{\eta} = \min\{\eta_i, i = 1, \dots, n\}$ with $\eta_i = b_i^2 / d_i$. The variance matrix $\mathbf{Q}_{\hat{\delta}}$ satisfies*

$$\frac{1}{2} \underline{\eta} \mathbf{S} \leq \mathbf{Q}_{\hat{\delta}} \leq \frac{1}{2} \bar{\eta} \mathbf{S}, \quad \mathbf{S} = \tilde{\mathbf{C}}^\top \mathbf{M}^{-1/2} \widehat{\mathbf{U}} \Lambda_{n-1}^{-1} \widehat{\mathbf{U}}^\top \mathbf{M}^{-1/2} \tilde{\mathbf{C}} \quad (21)$$

where $\Lambda_{n-1} = \text{diag}(\lambda_i, i = 2, \dots, n) \in \mathbb{R}^{(n-1) \times (n-1)}$.

Proof: Define matrices $\bar{\boldsymbol{\beta}} = (\bar{\eta} \mathbf{D})^{1/2}$ and $\underline{\boldsymbol{\beta}} = (\underline{\eta} \mathbf{D})^{1/2}$ and

$$\mathbf{Q}_{\bar{\boldsymbol{\beta}}} = \int_0^\infty e^{A_2 t} \bar{\mathbf{B}}_2 \bar{\mathbf{B}}_2^\top e^{A_2^\top t} dt, \quad \mathbf{Q}_{\underline{\boldsymbol{\beta}}} = \int_0^\infty e^{A_2 t} \underline{\mathbf{B}}_2 \underline{\mathbf{B}}_2^\top e^{A_2^\top t} dt$$

with $\bar{\mathbf{B}}_2, \underline{\mathbf{B}}_2 \in \mathbb{R}^{(2n-1) \times n}$ such that

$$\bar{\mathbf{B}}_2 = \begin{bmatrix} \mathbf{0} \\ \mathbf{U}^\top \mathbf{M}^{-1/2} \bar{\boldsymbol{\beta}} \end{bmatrix}, \quad \underline{\mathbf{B}}_2 = \begin{bmatrix} \mathbf{0} \\ \mathbf{U}^\top \mathbf{M}^{-1/2} \underline{\boldsymbol{\beta}} \end{bmatrix}.$$

From the definition of $\bar{\boldsymbol{\beta}}$ and $\underline{\boldsymbol{\beta}}$ and $\underline{\eta} d_i \leq b_i^2 = \eta_i d_i \leq \bar{\eta} d_i$ for all the nodes, it yields

$$\underline{\eta} \text{diag}(d_i) = \underline{\boldsymbol{\beta}} \underline{\boldsymbol{\beta}}^\top \leq \tilde{\mathbf{B}} \tilde{\mathbf{B}}^\top = \text{diag}(b_i^2) \leq \bar{\boldsymbol{\beta}} \bar{\boldsymbol{\beta}}^\top = \bar{\eta} \text{diag}(d_i).$$

which leads to

$$\underline{\mathbf{B}}_2 \underline{\mathbf{B}}_2^\top \leq \mathbf{B}_2 \mathbf{B}_2^\top \leq \bar{\mathbf{B}}_2 \bar{\mathbf{B}}_2^\top$$

By Theorem 3.4, we further obtain

$$\mathbf{Q}_{\underline{\boldsymbol{\beta}}} \leq \mathbf{Q}_{\hat{x}} \leq \mathbf{Q}_{\bar{\boldsymbol{\beta}}}. \quad (22)$$

Following [21, Lemma 4.2], we derive the explicit formula of $\mathbf{Q}_{\underline{\boldsymbol{\beta}}}$ and $\mathbf{Q}_{\bar{\boldsymbol{\beta}}}$ by solving the corresponding Lyapunov equations respectively,

$$\mathbf{Q}_{\underline{\boldsymbol{\beta}}} = \begin{bmatrix} \frac{1}{2} \underline{\eta} \Lambda_{n-1}^{-1} & \mathbf{0} \\ \mathbf{0} & \frac{1}{2} \underline{\eta} \mathbf{I} \end{bmatrix}, \quad \mathbf{Q}_{\bar{\boldsymbol{\beta}}} = \begin{bmatrix} \frac{1}{2} \bar{\eta} \Lambda_{n-1}^{-1} & \mathbf{0} \\ \mathbf{0} & \frac{1}{2} \bar{\eta} \mathbf{I} \end{bmatrix}.$$

With these explicit formulas and (18) and the form in (20), we obtain (21). \square

Based on this Lemma, we have the following theorem.

Theorem 3.7 Consider CREP Φ in Definition 3.2. It holds that

(1) each element of the vector \mathbf{f} and the value Φ are in the interval $[0, 1]$;

(2) if the second smallest eigenvalue of the matrix \mathbf{L}_c at the synchronous state decreases to zero, then the metric Φ increases to one.

Proof: (1) At a synchronous state, when the strength of the disturbances vary from zero to infinity, the variance σ_ω^2 of the frequencies at the nodes and σ_δ^2 in the lines vary from zero to infinity. It follows from Definition 3.2 for f_{δ_k} and f_{ω_k} , the values of Φ lies in the interval $[0, 1]$.

(2) By the definition in (11), f_{δ_k} decreases to one as the variance σ_{δ_k} increases to infinity. With the bounds of the matrix $\mathbf{Q}_{\hat{\delta}}$ in Lemma 3.6, we only need to prove that as the second smallest eigenvalue decreases to zero, there is at least one diagonal element of the matrix \mathbf{S} that increases to infinity. The incidence matrix of the graph is written into $\mathbf{C} = [\mathbf{c}_1 \ \mathbf{c}_2 \ \cdots \ \mathbf{c}_m]$, where \mathbf{c}_k describes the indices of the two nodes connected by line e_k . Without loss of generality, assume the line e_k connects nodes i and j and the direction of this line is from node i to j . Then, the i -th and j -th element of the vector \mathbf{c}_k are $c_{ik} = 1$ and $c_{jk} = -1$, respectively and the other elements all equal to zero. From the definition of the matrix \mathbf{S} in Lemma 3.6, we obtain the diagonal elements of \mathbf{S} ,

$$s_{kk} = \sum_{q=1}^{n-1} \lambda_{q+1}^{-1} (m_i^{-1/2} u_{i,q+1} - m_j^{-1/2} u_{j,q+1})^2, \quad k = 1, 2, \dots, m,$$

where $u_{i,q+1}$ and $u_{j,q+1}$ are the i -th and j -th element of the vector \mathbf{u}_{q+1} . Here \mathbf{u}_{q+1} is the $(q+1)$ -th column of the matrix \mathbf{U} defined in Lemma 3.3. Because \mathbf{u}_2 is a column of the orthogonal matrix \mathbf{U} , there exists i, j with $i \neq j$ such that $m_i^{-1/2} u_{i,2} \neq m_j^{-1/2} u_{j,2}$, thus s_{kk} increases to infinity as the second smallest eigenvalue λ_2 decreases to zero. \square

This theorem indicates that CREP Φ fully reflects the size of the basin of attraction of a stable synchronous state. In fact, it is known that as the power loads increases or the line capacities decreases, the synchronous state $((\delta^*)^\top, \mathbf{0})^\top$ moves to the boundary $\partial\Theta$ and both the second smallest eigenvalue λ_2 of \mathbf{L}_c and the size of the basin of attraction decrease. For the system (1), the number of eigenvalues of its system matrix \mathbf{A} with positive real part equals to the number of negative eigenvalues of \mathbf{L}_c [27]. Thus, when the secondary smallest eigenvalue of \mathbf{L}_c decreases to zero, the stable synchronous state gradually disappears, which means the basin of attraction disappears. Clearly, this is captured by CREP Φ which increases to one in this case. This theorem also demonstrates that CREP fully reflects the phenomena

that if the synchronous state is close to the boundary, a very small disturbance may lead to desynchronization.

To illustrate the procedure for calculating CREP and its characteristics, we apply it to the *Single Machine Infinite Bus* (SMIB) model with Gaussian disturbances,

Example 3.8 Consider the SMIB model with Gaussian disturbances,

$$\begin{aligned} \dot{\delta}(t) &= \omega(t), \\ M\dot{\omega}(t) &= P - D\omega(t) - K \sin \delta(t) + b\omega(t). \end{aligned}$$

Assume $P \leq K$, obviously, an equilibrium point is $(\delta^*, \omega^*) = (\arcsin P/K, 0)$. Linearising the system at the equilibrium point, we obtain a Gaussian stochastic process with system matrix and input matrix

$$\mathbf{A} = \begin{bmatrix} 0 & 1 \\ -M^{-1}l_c & -M^{-1}D \end{bmatrix}, \quad \mathbf{B} = \begin{bmatrix} 0 \\ M^{-1}b \end{bmatrix}$$

where $l_c = K \cos \delta^* = \sqrt{K^2 - P^2}$. By solving the following Lypunov equation,

$$\mathbf{A}\mathbf{Q} + \mathbf{Q}\mathbf{A}^\top + \mathbf{B}\mathbf{B}^\top = \mathbf{0},$$

we obtain the variance matrix in the invariant probability distribution of the stochastic process,

$$\mathbf{Q} = \begin{bmatrix} \frac{b^2}{2D\sqrt{K^2 - P^2}} & 0 \\ 0 & \frac{b^2}{2MD} \end{bmatrix}.$$

With this variance matrix and the equilibrium point as the expectation, the critical probability f_δ and f_ω are calculated according to Definition 3.2. Clearly, f_ω depends on the inertia and the damping of the synchronous machines and the strength of the disturbance while independent of the line capacity K and the load P . However, the dependence of f_δ on the system parameters is relatively complex.

It is clear that f_δ is independent of the inertia. Fig. 1 shows the trend of f_δ as the system parameters changes. In particular, as the load P increases to the line capacity, the basin of attraction of the equilibrium $(\delta^*, 0)$ gradually disappears. This is fully confirmed by f_δ , which increases to one. In Section 5, the Braess' paradox will be revisited with the proposed metric, where new findings will be presented.

4 The optimization framework

The proposed metric CREP actually quantifies the risk that the state escape from the critical set Θ . By minimizing this metric with the system parameters as the

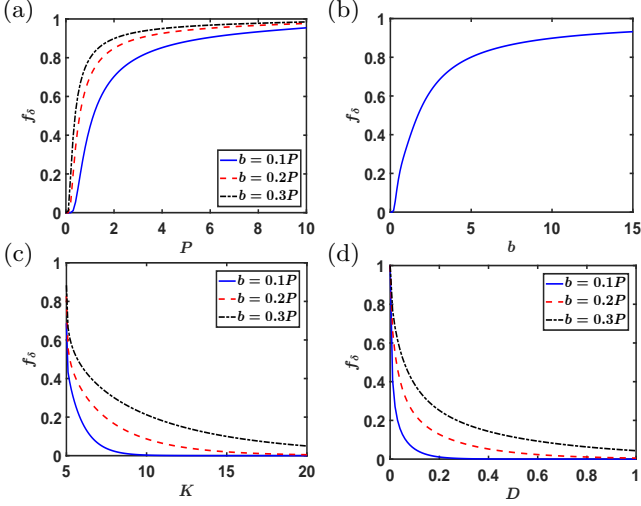


Fig. 1. The dependence of f_δ on the system parameters in SMIB model.

decision variables, this risk can be decreased, thus increasing the transient stability. For this minimization, we introduce an optimization framework with the choice of the decision variables as the line capacities, the power generations, the inertia coefficients and the damping coefficients,

$$\min_{\theta} \Phi = \|\mathbf{f}\|_\infty, \quad (23)$$

$$\text{s.t. } (2), (6), (11), (12), (14), (18), (19),$$

$$|\delta_i^* - \delta_j^*| \leq \pi/2, (i, j) \in \mathcal{E}, \quad (24)$$

$$\mathbf{g}(\theta) \leq 0, \quad (25)$$

where θ denotes the selected decision variable, $\mathbf{g}(\theta) \leq 0$ denotes the constraint on the selected decision variables. If only the rotor angle stability is considered, the objective function is replaced by Φ_δ . Similarly, if suppressing the frequency fluctuations is the main purpose, the objective function is replaced by Φ_ω . We remark that the constraints (24) cannot be neglected because there may be many equilibrium points for the system (1) that are not in the set Θ [25] and unexpected unstable synchronous state may be obtained if these constraints are neglected.

If the power generation are selected as the decision variables, which is usually optimized in the tertiary frequency control, the constraints (25) are replaced by

$$0 = P_t - \sum_{i \in \mathcal{V}_g} P_i, \quad (26a)$$

$$\underline{P}_i \leq P_i \leq \bar{P}_i, i \in \mathcal{V}_g, \quad (26b)$$

where P_t is the total power load, $\mathcal{V}_g \subset \mathcal{V}$ denotes the set of power generations, \underline{P}_i and \bar{P}_i are the lower bound and upper bound of the power generation respectively. Note that the power load at a node may also be selected

as a decision variable, the form of the constraints are the same as (26).

If the inertia of the synchronous machines are the decision variables such that $\theta = \text{col}(m_i) \in \mathbb{R}^n$, the constraints (25) are replaced by

$$0 = M_t - \sum_{i=1}^n m_i, \quad (27a)$$

$$\underline{m}_i \leq m_i \leq \bar{m}_i, i = 1, \dots, n, \quad (27b)$$

where M_t denotes the total amount of inertia and \underline{m}_i and \bar{m}_i are the lower bounds and upper bounds of inertia coefficients respectively.

Similarly, if the damping coefficients are selected as decision variables such that $\theta = \text{col}(d_i) \in \mathbb{R}^n$, the constraints (25) are then replaced by

$$0 = D_t - \sum_{i=1}^n d_i, \quad (28a)$$

$$\underline{d}_i \leq d_i \leq \bar{d}_i, i = 1, \dots, n, \quad (28b)$$

where D_t denotes the total amount of damping and \underline{d}_i and \bar{d}_i are the lower bound and upper bound of the damping coefficient at node i respectively.

If the line capacities of the lines are selected as decision variables, i.e., $\theta = \text{col}(l_{i,j}) \in \mathbb{R}^m$ with $(i, j) \in \mathcal{E}$, the constraints (25) are replaced by

$$0 = L_t - \sum_{(i,j) \in \mathcal{E}} l_{i,j}, \quad (29a)$$

$$\underline{l}_{i,j} \leq l_{i,j} \leq \bar{l}_{i,j}, (i, j) \in \mathcal{E}, \quad (29b)$$

where L_t is the total available line capacities and $\underline{l}_{i,j}$ and $\bar{l}_{i,j}$ are the lower bound and the upper bound of the capacity of line $(i, j) \in \mathcal{E}$ respectively.

When the objective function in (23) is replaced by $\Phi_\omega = \|\mathbf{f}_\omega\|_\infty$, the frequency fluctuations are minimized by tuning the system parameters. For this minimization problem, we have the following proposition.

Proposition 4.1 Consider the metric $\Phi_\omega = \|\mathbf{f}_\omega\|_\infty$ with \mathbf{f}_ω defined in Definition 3.2. Minimizing $\|\mathbf{f}_\omega\|_\infty$ is equivalent to minimizing $\|\sigma_\omega^2\|_\infty$.

Proof: It holds

$$\begin{aligned} \frac{df_{\omega_k}}{d\sigma_{\omega_k}} &= - \int_{-\epsilon}^{\epsilon} \frac{1}{\sqrt{2\pi}\sigma_{\omega_k}^2} e^{-\frac{z^2}{2\sigma_{\omega_k}^2}} \left(\frac{z^2}{\sigma_{\omega_k}^2} - 1 \right) dz \\ &= \frac{1}{\sqrt{2\pi}\sigma_{\omega_k}^2} z e^{-\frac{z^2}{2\sigma_{\omega_k}^2}} \Big|_{z=-\epsilon}^{z=\epsilon} = \frac{2\epsilon}{\sqrt{2\pi}\sigma_{\omega_k}^2} e^{-\frac{\epsilon^2}{2\sigma_{\omega_k}^2}} > 0. \end{aligned}$$

The value f_{ω_i} is monotonically increasing with respect to the standard variance σ_{ω_i} . Thus, minimizing $\|\mathbf{f}_\omega\|_\infty$ is equivalent to minimizing $\|\sigma_\omega^2\|_\infty$. \square

With this proposition, the objective function can be further replaced by $\|\sigma_\omega^2\|_\infty$. We remark that this is different from minimizing the \mathcal{H}_2 norm as in the optimization framework (B.1) where the objective function is the sum of the frequency variances at all the nodes.

Note that in the constraints (26), (27), (28) and (29), the upper bound may equal to the lower bound, in which case the corresponding decision variables become constants. The constraints (24) restrict the synchronous state in the domain (7). Because the synchronous state may not exist, there may be no solutions for the optimization problem in that case.

5 Case study

In this section, we evaluate the performance of the proposed metric on assessing the transient stability and the optimization framework on enhancing the transient stability of a system with network topology as shown in Fig. 2. In this model, all the buses are assumed to be synchronous machines. There are 39 nodes and 46 lines. The nodes with even numbers are connected to power generators and the other nodes are connected to power loads, which are denoted by blank nodes and grey nodes respectively in Fig. 2.

Because the solution of the optimization problem with objective (23) is sensitive to the parameter ϵ , i.e., if it is too large, the phase difference will often first hit the boundary, while if it is too small, the frequency component will often first hit the boundary. Due to difficulty in the configuration, we first study the metric Φ regardless the frequency fluctuations, which lead to $\Phi = \Phi_\delta$, and then study it without boundary trigger of the phase differences, which leads to $\Phi = \Phi_\omega$. For the former case, we only need to evaluate the performance of the metric $\Phi_\delta = \|\mathbf{f}_\delta\|_\infty$ and the corresponding optimization framework. For the latter one, we evaluate $\Phi_\omega = \|\mathbf{f}_\omega\|_\infty$ and its corresponding optimization framework. In particular, we revisit the Braess' paradox, in which according to earlier studies using different metrics the stability may be decreased when a new line is added or the line capacity of an existing line is increased.

The phase cohesiveness measured either by $\|\mathbf{y}_\delta^*\|_\infty$ or the order parameter at the synchronous state and the \mathcal{H}_2 norm of the system with stochastic input may be considered as metrics for optimal network design[7,18], for which the corresponding optimization frameworks are introduced in the Appendix. Here, we compare the performance of these optimization frameworks to that of the proposed framework in this paper. The corresponding optimization problems are solved by the Genetic Al-

gorithm method using Matlab. The bound constraints (26b-29b) of the decision variables are not considered.

To show the results intuitively, the mean first hitting time \bar{t}_ℓ of $\mathbf{y}(t)$ to the boundary $\partial\Theta_y$ is used to indicate the enhancement of the transient stability in these evaluations, which is calculated statistically by the Monte-Carlo method for the nonlinear system (4). The Euler-Maruyama method is applied to the system (4) with the initial condition $(\delta(0), \omega(0)) = (\delta^*, \mathbf{0})$ and simulation time $T = 10^5$. The total number of samples for calculating the mean first hitting time is $N = 10^5$ and the time step for the simulation is $\Delta t = 10^{-3}$.

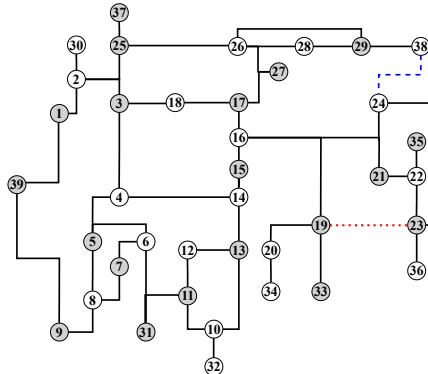


Fig. 2. A network for case study. The grey nodes represent power loads and the blank nodes represent power generations.

In subsection 5.1, we investigate the dependence of Φ_δ on the system parameters and the relationship between Φ_δ and \bar{t}_ℓ . The performance of minimizing Φ_δ and the revisit of Braess' paradox are also described in this subsection. In subsection 5.2, we introduce the dependence of Φ_ω on the system parameters and the performance of minimizing Φ_ω .

5.1 The metric Φ_δ

To understand the dependence of the metric Φ_δ on the system parameters and the performance of proposed optimization framework, we focus the systems with the following 5 configurations of system parameters respectively, where the decision variables may be the power generation, the line capacities of all the lines, the inertia and the damping coefficients of the synchronous machines at all the nodes separately.

- (1) The parameters selected as decision variables are set identically. For example, when the power generation is selected as decision variables, we set all the power generation identically with total power supply P_T in these systems, i.e., $P_i = P_T/N_g$ where N_g is the total number of generators and also is the dimension of the decision variables. We mention the models with this parameter configuration as *initial models* for simplicity;

- (2) The parameters selected as decision variables are set to the solution of the optimization problems minimizing Φ_δ . For example, when the power generation are selected as decision variables, the values of the power generation is set to the solution of the optimization problems with objective Φ_δ .
- (3) The parameters selected as decision variables are set to the solution of the optimization problems minimizing $\text{tr}(\mathbf{Q}_\delta)$ which actually is the \mathcal{H}_2 norm of the system (9); See (B.1) for the corresponding optimization problems;
- (4) The parameters selected as decision variables are set to the solution of the optimization problems minimizing $\|\mathbf{y}_\delta^*\|_\infty$, which measures the cohesiveness of the phases. See (B.2) for the corresponding optimization problems.
- (5) The parameters selected as decision variables are set to the solution of the optimization problems maximizing the order parameter, which is often used to study the level of the synchronization of complex network systems. See (B.4) for the corresponding optimization problems.

We set $b_i = 0.5\sqrt{i+1}$. If a parameter is not selected as a decision variable, it is set as in Table 1. For example, if the power generation are selected as decision variables, then we set the other variables as shown in Table 1, i.e., $l_{i,j} = 20$, $M_i = 0.08i$, $d_i = 0.2 \times (42 - i)$. Specially, when studying the dependence of the metric Φ_δ and the mean first hitting time \bar{t}_e on the power generation and loads, we set the power loads identically with total amount of power P_t . In the Monte-Carlo methods for the simulations of the system (4), the first hitting time t_e is recorded when there are lines in which the phase differences exit the set Θ_δ regardless of the deviations of the frequencies. The initial models are used for comparing the performance of the 4 optimization frameworks.

5.1.1 The dependence of Φ_δ on the system parameters

The dependence of \bar{t}_e and Φ_δ on the parameters P_t , L_t , M_t and D_t are shown in Fig. 3. The findings from these figures are summarized below.

First, by comparing the trends of $\Phi_\delta = \|\mathbf{f}_\delta\|_\infty$ as these parameters change in Fig. 3(a-d) with those of \bar{t}_e in Fig. 3(e-h), it can be observed that when the metric $\|\mathbf{f}_\delta\|_\infty$ increases, \bar{t}_e decreases. This demonstrates that CREP fully reflects the trends of the mean first hitting time, and shows the ability of effectively assessing the transient stability in terms of the mean first hitting time.

Second, it is found from Fig. 3(a,b,d) that $\Phi_\delta = \|\mathbf{f}_\delta\|_\infty$ decreases as L_t and D_t increase respectively while increases as P_t increases in all the 5 models. This is practical. In particular, it is shown in Fig. 3(c) that when the inertia increases, $\|\mathbf{f}_\delta\|_\infty$ decreases significantly. This

demonstrates that increasing the inertia is also beneficial to the rotor angle stability, which is consistent with the findings from the explicit formula of the variance matrix of the phase differences for star networks in [24]. This is because a large inertia accelerates the propagation of the disturbances from a node to the other nodes. It is remarked that with the assumption of uniform disturbance-damping ratio, i.e., $b_i^2/d_i = \eta$ for all the nodes, the variance of the phase differences is independent of the inertia [21].

We remark that the objectives $\|\mathbf{y}_\delta^*\|_\infty$ in (B.2) and the order parameter (B.4) are independent of the inertia and damping coefficients of synchronous machines. Thus, when the inertia and the damping coefficients are selected as decision variables, the values of \bar{t}_e will not be changed. This is shown in Fig. 3(g,h) where the curves of the mean first hitting time in the initial model and the ones with system parameters setting to the solutions of maximizing the order parameter γ and minimizing $\|\mathbf{y}_\delta^*\|_\infty$ coincide.

5.1.2 Performance of minimizing Φ_δ

We compare the performances of the optimization frameworks, i.e., the ability on increasing the mean first hitting time \bar{t}_e . In Fig. 3(e-h), it is clearly shown that \bar{t}_e with system parameters optimized by the proposed optimization framework, that are denoted by red dotted lines, is much larger than all the others. This demonstrates that minimizing Φ_δ is more effective on increasing the transient stability than optimizing all the other metrics. *This also confirms that for enhancing the transient stability, it is insufficient to suppress the fluctuations only.* Obviously, when the strength of the disturbance decreases to zero which leads σ_δ^2 to zero, the effectiveness gradually reduces to that of the optimization framework (B.2).

5.1.3 Revisit of the Braess' paradox with Φ_δ

If a new line is added or the capacity of a line increases, its influences can be evaluated from the changes of the linear stability measured by the absolute values of the real parts of the non-zero eigenvalues of the system matrix \mathbf{A} in (9) or the order parameter γ defined in (B.3). We denote the smallest absolute value of the real parts of the nonzero eigenvalues by $\min\{|\text{Re}(\mu_i)|\}$ where μ_i denotes the non-zero eigenvalues of \mathbf{A} . A Braess' paradox occurs if $\min\{|\text{Re}(\mu_i)|\}$ or the order parameter γ decrease when a new line is added or the capacity of a line increases. Here, on the network shown in Fig. 1, we study the performance of Φ_δ on identifying a Braess' paradox and compare it with those of the linear stability and the order parameter. We set $b_i = 0.09i$ and set the other parameters as in Table 1. We show in Table 2 the values of \bar{t}_e , $\|\mathbf{f}_\delta\|_\infty$, $\min\{|\text{Re}(\mu_i)|\}$ and γ , where the confidence intervals of \bar{t}_e with confidence level 95% are $[\bar{t}_e - t_c, \bar{t}_e + t_c]$ with $t_c \leq 2s$ in all the 4 cases.

Let us first focus on the changes of these metrics after a new line is added, i.e., either line (19, 23) in case 2 or (24, 38) in case 3. It is shown in Table 2 that after adding line (19, 23), $\min\{|\operatorname{Re}(\mu_i)|\}$ and γ increase from 0.2833 to 0.3179 and 0.9663 to 0.9666 respectively, which indicate the stability is increased. While, $\|\mathbf{f}_\delta\|_\infty$ increases from 4.383×10^{-6} to 1.419×10^{-5} and \bar{t}_e decreases from 195.14s to 148.94s, both indicate the stability is decreased. Clearly, this conflicts with the result by $\min\{|\operatorname{Re}(\mu_i)|\}$ and γ . Conversely, in case of adding line (24, 38), a Braess' paradox is identified with respect to $\min\{|\operatorname{Re}(\mu_i)|\}$ and γ , which decrease from 2.833 to 2.832 and from 0.9663 to 0.9652 respectively. In contrast, with the metric $\|\mathbf{f}_\delta\|_\infty$, which decreases from 4.383×10^{-6} to 3.393×10^{-6} , and the metric \bar{t}_e , which increases from 195.14s to 241.51s, it is identified that the new added line increases the stability.

We next study the changes of these metrics after increasing the line capacity of (22, 35) by comparing the results of case 1 and case 4 in Table 2. It is seen that after increasing the line capacity, $\min\{|\operatorname{Re}(\mu_i)|\}$ and the order parameter increase from 0.2833 to 0.3103 and from 0.9663 to 0.9666 respectively, both indicate that increasing the line capacity of (22, 35) is beneficial to the stability. However, the metric $\|\mathbf{f}_\delta\|_\infty$ increases from 4.383×10^{-6} to 4.967×10^{-6} and the mean first hitting time decreases from 195.14s to 188.11s, which indicate that stability decreases, thus a Braess' paradox occurs.

In words, *whether a Braess' paradox occurs depends on the metric used for the stability*. The proposed metric that involves the roles of all the system parameters and the strength of disturbances provides a more practical tool to identify a Braess' paradox.

5.2 The metric Φ_ω

In this subsection, we study the dependence of the metric $\Phi_\omega = \|\mathbf{f}_\omega\|_\infty$ on the system parameters and the performance of the optimization framework. We focus on the mean first hitting time \bar{t}_e when the frequencies exit the range Θ_ω and $\|\mathbf{f}_\omega\|_\infty$ in the systems with the following 3 configurations of system parameters.

- (1) The parameters selected as decision variables are set identically. The model with this parameter configuration are also called *initial models* and used for comparison as in the previous subsection.
- (2) The parameters selected as decision variables are set to the solution of the optimization problems minimizing $\operatorname{tr}(\mathbf{Q}_\omega)$.
- (3) The parameters selected as decision variables are set to the solution of the optimization problems minimizing $\|\sigma_\omega^2\|_\infty$. For the optimization problems, see (B.1) with the objective replaced by $\|\sigma_\omega^2\|_\infty$.

We set $b_i = 5i \times 10^{-4}$, which is much smaller than the setting in Subsection 5.1. The parameters that are not

selected as decision variables are set to the values in Table 1. Note that minimizing $\|\sigma_\omega^2\|_\infty$ is equivalent to minimizing $\|\mathbf{f}_\omega\|_\infty$ based on Proposition 4.1. As in the previous subsection, when studying the impact of the power generation and loads on the metric $\|\mathbf{f}_\omega\|_\infty$, we select all the power generation as decision variables and set the power load identically with the total amount P_t . We set $\epsilon = 0.02$ to calculate $\|\mathbf{f}_\omega\|_\infty$ and \bar{t}_e in the simulations of (4). In the Monte-Carlo methods for the simulations of the system (4), the first hitting time is recorded when there are nodes at which the frequencies exit the range Θ_ω regardless of the fluctuations of the phase differences. Note that in all the simulations, because the strengths of the disturbances are much smaller than those in Subsection 5.1, the phase differences in all the lines remain in the range Θ_δ in the simulations. In other words, the frequencies always hit the boundary of Θ_ω first. The simulation results are shown in Fig. 4.

5.2.1 The dependence of Φ_ω on the system parameters

It is observed from Fig. 4 that $\|\mathbf{f}_\omega\|_\infty$ increases as P_t increases and decreases as L_t increases. This is because either increasing P_t or decreasing L_t will decrease the weight $l_{i,j} \cos(\delta_i^* - \delta_j^*)$ for all $(i, j) \in \mathcal{E}$, which decelerates the propagation of disturbances from a node to the others. Note that accelerating the propagation of the disturbances in a network with heterogeneous strength of disturbances is beneficial to decrease $\|\sigma_\omega^2\|_\infty$ which further decreases $\|\mathbf{f}_\omega\|_\infty$. This is consistent with the theoretical analysis with explicit formulas of the variance matrix in special networks that includes star networks and complete networks in [24].

From Fig. 4(c-d), it is seen that as M_t and D_t increase, $\|\mathbf{f}_\omega\|_\infty$ decreases respectively. This is consistent with the analysis in [21] and [24] on the dependence of σ_ω^2 on the inertia and damping coefficients.

Comparing the figures of \bar{t}_e and $\|\mathbf{f}_\omega\|_\infty$ in Fig.4(a-d) and (e-h), we find that the trend of $\|\mathbf{f}_\omega\|_\infty$ fully reflects the dependence of \bar{t}_e on the system parameters. Thus, CREP characterizes the mean first hitting time consequently assesses the transient stability of power systems.

5.2.2 Performance of minimizing Φ_ω

By comparing the curves of \bar{t}_e in Fig. 4(e-h), the mean first hitting time when $\|\mathbf{f}_\omega\|_\infty$ is minimized is the largest one among the three metrics. This demonstrates that the proposed optimization framework is the most effective on increasing the transient stability.

In contrast, it is surprising found from Fig. 4(c-d) and (g-h) that the curves of $\|\mathbf{f}_\omega\|_\infty$ and \bar{t}_e in the initial model and the model where $\operatorname{tr}(\mathbf{Q}_\omega)$ are minimized, almost overlap. This indicates that by minimizing $\operatorname{tr}(\mathbf{Q}_\omega)$ with either the inertia M_i or the damping D_i as decision variables, the stability can hardly be improved.

Table 1

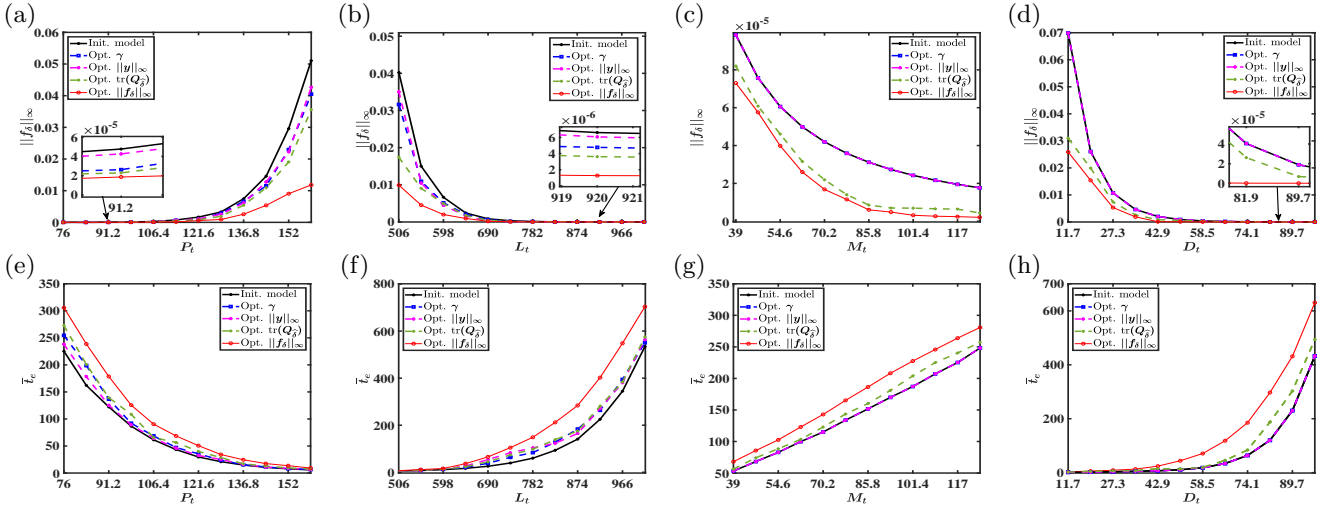
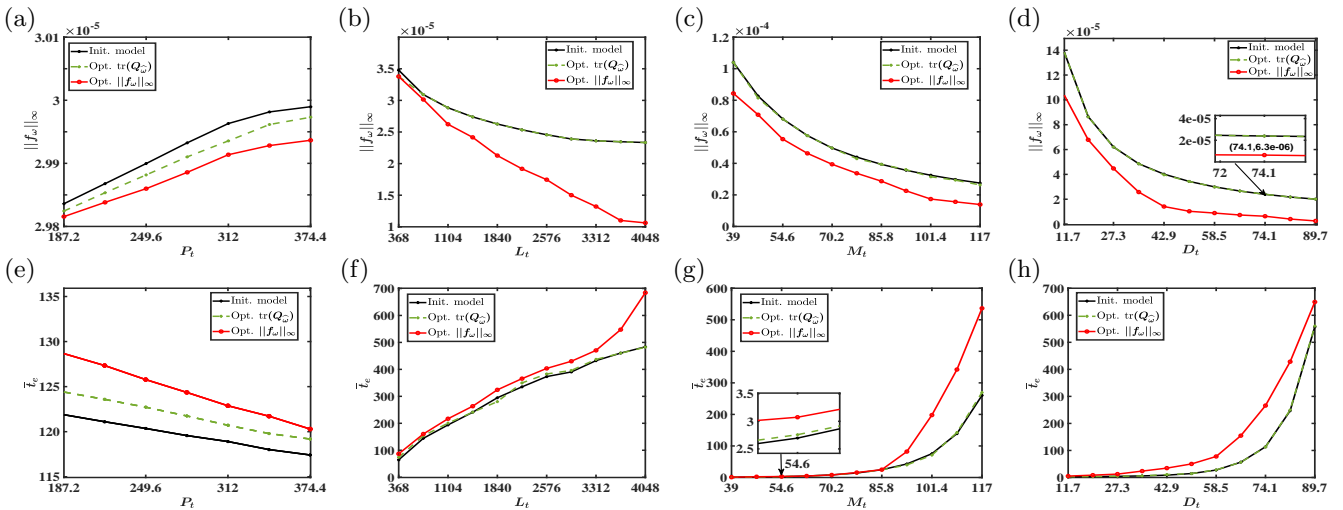
Configuration of the system parameters of evaluating the performance of $\|f_\delta\|_\infty$.

$P_{2i-1}, i = 1, \dots, 20$	P_2	$P_{2i}, i = 2, \dots, 19$	$l_{i,j}, (i,j) \in \mathcal{E}$	m_i	d_i
-4	8	4	20	$0.08i$	$0.2 \times (42 - i)$

Table 2

Comparison of $\|f_\delta\|$ with $\min\{|\operatorname{Re}\mu_i|\}$ and the order parameters on identifying the Braess' paradox. The confidence intervals of \bar{t}_e with confidence level 95% are $[\bar{t}_e - t_c, \bar{t}_e + t_c]$ with $t_c \leq 2s$ in all the 4 cases.

Case	Added line	Line capacity		\bar{t}_e	$\ f_\delta\ _\infty$	$\min \operatorname{Re}(\mu_i) $	γ
		(22, 35)	others				
1	-	20	20	195.14s	4.383×10^{-6}	0.2833	0.9663
2	(19, 23)	20	20	148.94s	1.419×10^{-5}	0.3179	0.9666
3	(24, 38)	20	20	241.51s	3.393×10^{-6}	0.2832	0.9652
4	-	30	20	188.11s	4.967×10^{-6}	0.3103	0.9666

Fig. 3. The dependence of \bar{t}_e and $\|f_\delta\|_\infty$ on the parameters P_t , L_t , M_t and D_t in the models with the 5 configurations of parameters.Fig. 4. The dependence of \bar{t}_e and $\|f_\omega\|_\infty$ on the parameters P_t , L_t , M_t and D_t in the models with the 3 configurations of parameters.

6 Conclusion

Based on the theory of the invariant probability distribution of a stochastic process driven by Brownian motion, we have proposed a metric named CREP, which involves all the system parameters and reflects the size of the basin of attraction, to assess the transient stability. An optimization framework minimizing CREP with the system parameters as decision variables was formulated. The mean first hitting time of the state hitting the boundary of a critical set, can be significantly increased by this approach, which intuitively shows the strong potential of our approach in enhancing the transient stability.

Future study will be on efficient algorithms for solving the corresponding optimization problems and theoretical analysis of the transient stability enhancement of power systems with non-Gaussian noise [16]. Extensions of the method for robustness improvement of the other nonlinear systems with continuously occurring disturbances will also be investigated.

A The invariant probability distribution and \mathcal{H}_2 norm

Consider a linear time-invariant system,

$$\dot{\mathbf{x}} = \mathbf{A}\mathbf{x} + \mathbf{B}\mathbf{v}, \quad (\text{A.1a})$$

$$\mathbf{y} = \mathbf{C}\mathbf{x}, \quad (\text{A.1b})$$

where $\mathbf{x} \in \mathbb{R}^{n_x}$, $\mathbf{A} \in \mathbb{R}^{n_x \times n_x}$ is Hurwitz, $\mathbf{B} \in \mathbb{R}^{n_x \times n_v}$, $\mathbf{C} \in \mathbb{R}^{n_y \times n_x}$, the input is denoted by $\mathbf{v} \in \mathbb{R}^{n_v}$ and the output of the system is denoted by $\mathbf{y} \in \mathbb{R}^{n_y}$. The squared \mathcal{H}_2 norm of the transfer matrix \mathbf{G} of the mapping $(\mathbf{A}, \mathbf{B}, \mathbf{C})$ from the input \mathbf{v} to the output \mathbf{y} is defined as

$$\|\mathbf{G}\|_2^2 = \text{tr}(\mathbf{B}^T \mathbf{Q}_o \mathbf{B}) = \text{tr}(\mathbf{C} \mathbf{Q}_c \mathbf{C}^T), \quad (\text{A.2a})$$

$$\mathbf{Q}_o \mathbf{A} + \mathbf{A}^T \mathbf{Q}_o + \mathbf{C}^T \mathbf{C} = \mathbf{0}, \quad (\text{A.2b})$$

$$\mathbf{A} \mathbf{Q}_c + \mathbf{Q}_c \mathbf{A}^T + \mathbf{B} \mathbf{B}^T = \mathbf{0}, \quad (\text{A.2c})$$

where $\text{tr}(\cdot)$ denotes the trace of a matrix, $\mathbf{Q}_o, \mathbf{Q}_c \in \mathbb{R}^{n_x \times n_x}$ are the *observability Grammian* of (\mathbf{C}, \mathbf{A}) and *controllability Grammian* of (\mathbf{A}, \mathbf{B}) respectively [6,20]. When the input \mathbf{v} is modelled by Gaussian white noise, the distribution of the state \mathbf{x} and the output \mathbf{y} are also Gaussian. Denote then for all $t \in T$, $\mathbf{x}(t) \in G(\mathbf{m}_x(t), \mathbf{Q}_x(t))$ with $\mathbf{Q}_x(t) \in \mathbb{R}^{n_x \times n_x}$ and $\mathbf{y}(t) \in G(\mathbf{m}_y(t), \mathbf{Q}_y(t))$ with $\mathbf{Q}_y(t) \in \mathbb{R}^{n_y \times n_y}$. Because the matrix \mathbf{A} is Hurwitz, there exists an invariant probability distribution of this linear stochastic system with the representation and properties

$$\begin{aligned} \mathbf{0} &= \lim_{t \rightarrow \infty} \mathbf{m}_x(t), \quad \mathbf{0} = \lim_{t \rightarrow \infty} \mathbf{m}_y(t), \\ \mathbf{Q}_x &= \lim_{t \rightarrow \infty} \mathbf{Q}_x(t), \quad \mathbf{Q}_y = \lim_{t \rightarrow \infty} \mathbf{Q}_y(t), \end{aligned}$$

where the variance matrices are

$$\mathbf{Q}_x = \int_0^{+\infty} \exp(\mathbf{A}t) \mathbf{B} \mathbf{B}^T \exp(\mathbf{A}^T t) dt, \quad \mathbf{Q}_y = \mathbf{C} \mathbf{Q}_x \mathbf{C}^T.$$

Here \mathbf{Q}_x is the unique solution of the Lyapunov matrix function (A.2c).

B The traditional optimization frameworks

In this section, we present the traditional metric for the optimal configuration of the system parameters, the \mathcal{H}_2 norm of the system (9), the phase cohesiveness and the order parameters for the level of the synchronization.

The \mathcal{H}_2 norm of the system (9) where the term $\mathbf{B}\mathbf{v}(t)$ is seen as input to the system, is actually the trace of matrix \mathbf{Q}_x . To minimize this norm, the optimization framework is

$$\min_{\boldsymbol{\theta}} \text{tr}(\mathbf{Q}_x) \quad (\text{B.1})$$

$$\text{s.t. (2), (6),(14), (18), (19), (24), (25).}$$

If the maximum of the variance of the phase angle differences in the edges is minimized, the objective function is replaced by $\|\boldsymbol{\sigma}_\delta^2\|_\infty$ in (B.1). The decision variables $\boldsymbol{\theta}$ can be either the power generation, the inertia, the damping coefficients or the line capacities and the corresponding constraints (25) can be replaced by the ones in (26), (27), (28) and (29) respectively.

The optimization framework for improving the phase cohesiveness is

$$\min_{\boldsymbol{\theta}} \|\mathbf{y}_\delta^*\|_\infty, \quad (\text{B.2})$$

$$\text{s.t. (2), (6),(24),(25).}$$

The order parameter of couple phase oscillators is defined as

$$\gamma e^{i\phi} = \frac{1}{n} \sum_{j=1}^n e^{i\delta_j} \quad (\text{B.3})$$

where $i^2 = -1$ and δ_j is the phase at node j and $\gamma e^{i\phi}$ is the phase' centroid on the complex unit circle with the magnitude γ ranging from 0 to 1 [10]. In Section 5, the order parameter is maximized by solving the following optimization problem [18],

$$\max_{\boldsymbol{\theta}} \gamma = 1 - \|\boldsymbol{\delta}^*\|_2^2/n, \quad (\text{B.4})$$

$$\text{s.t (2),(24),(25).}$$

The decision variables $\boldsymbol{\theta}$ can be either the power generation or the line capacities and the corresponding constraints (25) can be replaced by the ones in (26) and (29)

respectively. In (B.2) and (B.4), because the inertia and the damping of the synchronous machines have no impacts on the synchronous state, these parameters cannot be configured in an optimal way by these frameworks.

References

- [1] H. D. Chiang, M.W. Hirsch, and F.F. Wu. Stability regions of nonlinear autonomous dynamical systems. *IEEE Trans. Autom. Control*, 33(1):16–27, jan 1988.
- [2] T. Coletta and P. Jacquod. Linear stability and the Braess paradox in coupled-oscillator networks and electric power grids. *Phys. Rev. E*, 93(3):032222, mar 2016.
- [3] R. Delabays, M. Tyloo, and Ph. Jacquod. The size of the sync basin revisited. *Chaos*, 27(10):103109, 2017.
- [4] F. Dörfler and F. Bullo. On the critical coupling for Kuramoto oscillators. *SIAM J. Appl. Dyn. Syst.*, 10(3):1070–1099, 2011.
- [5] F. Dörfler and F. Bullo. Synchronization in complex networks of phase oscillators: A survey. *Automatica*, 50(6):1539 – 1564, 2014.
- [6] J. C. Doyle, K. Glover, P. P. Khargonekar, and B. A. Francis. State-space solutions to standard H2 and H infinity control problems. *IEEE Trans. Autom. Control*, 34(8):831–847, Aug 1989.
- [7] M. Fazlyab, F. Dörfler, and V. M. Preciado. Optimal network design for synchronization of coupled oscillators. *Automatica*, 84:181 – 189, 2017.
- [8] M. M. Klosek-Dygas, B. J. Matkowsky, and Z. Schuss. Stochastic stability on nonlinear oscillators. *SIAM Journal on Applied Mathematics*, 48(5):1115–1127, 1988.
- [9] P. Kundur. *Power system stability and control*. McGraw-Hill, 1994.
- [10] Y. Kuramoto. *Chemical oscillations, waves and turbulence*. Springer, New York, 1984.
- [11] M. T. Lee and G. A. Whitmore. Threshold regression for survival analysis: Modeling event times by a stochastic process reaching a boundary. *Statistical Science*, 21(4):501–513, 2006.
- [12] P. J. Menck, J. Heitzig, J. Kurths, and H. Joachim Schellnhuber. How dead ends undermine power grid stability. *Nat. Commun.*, 5:3969, jun 2014.
- [13] P. J. Menck, J. Heitzig, N. Marwan, and Jürgen Kurths. How basin stability complements the linear-stability paradigm. *Nat. Phys.*, 9(2):89–92, jan 2013.
- [14] L. M. Pecora and T. L. Carroll. Master stability functions for synchronized coupled systems. *Phys. Rev. Lett.*, 80:2109–2112, Mar 1998.
- [15] B. K. Poolla, S. Bolognani, and F. Dörfler. Optimal placement of virtual inertia in power grids. *IEEE Trans. Autom. Control*, 62(12):6209–6220, 2017.
- [16] B. Schäfer, C. Beck, K. Aihara, D. Witthaut, and M. Timme. Non-Gaussian power grid frequency fluctuations characterized by Lévy-stable laws and superstatistics. *Nature Energy*, 3(2):119–126, 2018.
- [17] S. J. Skar. Stability of multi-machine power systems with nontrivial transfer conductances. *SIAM J. Appl. Math.*, 39(3):475–491, 1980.
- [18] P. S. Skardal, D. Taylor, and J. Sun. Optimal synchronization of complex networks. *Phys. Rev. Lett.*, 113:144101, Sep 2014.
- [19] E. Tegling, B. Bamieh, and D. F. Gayme. The price of synchrony: Evaluating the resistive losses in synchronizing power networks. *IEEE Trans. Control Netw. Syst.*, 2(3):254–266, Sept 2015.
- [20] R. Toscano. *Structured controllers for uncertain systems*. Springer-verlag, London, 2013.
- [21] Z. Wang, K. Xi, A. Cheng, H. X. Lin, A. C.M. Ran, J. H. van Schuppen, and C. Zhang. Synchronization of power systems under stochastic disturbances. *Automatica*, 151:110884, 2023.
- [22] D. Witthaut and M. Timme. Braess’s paradox in oscillator networks, desynchronization and power outage. *New J. Phys.*, 14(8):083036, aug 2012.
- [23] X. Wu, K. Xi, A. Cheng, H. X. Lin, and J. H. van Schuppen. Increasing the synchronization stability in complex networks. *Chaos: An Interdisciplinary Journal of Nonlinear Science*, 33(4), 04 2023. 043116.
- [24] X. Wu, K. Xi, A. Cheng, H. X. Lin, J. H. van Schuppen, and C. Zhang. Explicit formulas for the variance of the state of a linearized power system driven by Gaussian stochastic disturbances. *preprint in arXiv:2302.06326*, 2023.
- [25] K. Xi, J. L. A. Dubbeldam, and H. X. Lin. Synchronization of cyclic power grids: equilibria and stability of the synchronous state. *Chaos*, 27(1):013109, 2017.
- [26] K. Xi, J. L.A. Dubbeldam, H. X. Lin, and J. H. van Schuppen. Power-Imbalance Allocation Control of Power Systems-Secondary Frequency Control. *Automatica*, 92:72 – 85, 2018.
- [27] J. Zaborsky, G. Huang, T. C. Leung, and B. Zheng. Stability monitoring on the large electric power system. In *24th IEEE Conf. Decision Control*, volume 24, pages 787–798. IEEE, dec 1985.
- [28] J. Zaborszky, G. Huang, B. Zheng, and T. C. Leung. On the phase portrait of a class of large nonlinear dynamic systems such as the power system. *IEEE Trans. Autom. Control*, 33(1):4–15, jan 1988.
- [29] X. Zhang, S. Hallerberg, M. Matthiae, D. Witthaut, and M. Timme. Fluctuation-induced distributed resonances in oscillatory networks. *Sci. Adv.*, 5(7):eaav1027, 2019.
- [30] X. Zhang, D. Witthaut, and M. Timme. Topological determinants of perturbation spreading in networks. *Phys. Rev. Lett.*, 125:218301, 2020.